



CHAOTIC ATTRACTOR IN THE KURAMOTO MODEL

YURI L. MAISTRENKO*, OLEKSANDR V. POPOVYCH and
PETER A. TASS†

*Institute of Medicine and Virtual Institute of Neuromodulation,
Research Centre Jülich, 52425 Jülich, Germany*

**Institute of Mathematics, Academy of Sciences of Ukraine,
01601 Kyiv, Ukraine*

*†Department of Stereotaxic and Functional Neurosurgery,
University Hospital, 50924 Cologne, Germany*

Received December 22, 2004; Revised February 23, 2005

The Kuramoto model of globally coupled phase oscillators is an essentially nonlinear dynamical system with a rich dynamics including synchronization and chaos. We study the Kuramoto model from the standpoint of bifurcation and chaos theory of low-dimensional dynamical systems. We find a chaotic attractor in the four-dimensional Kuramoto model and study its origin. The torus destruction scenario is one of the major mechanisms by which chaos arises. L. P. Shilnikov has made decisive contributions to its discovery. We show also that in the Kuramoto model the transition to chaos is in accordance with the torus destruction scenario. We present the general bifurcation diagram containing phase chaos, Cherry flow as well as periodic and quasiperiodic dynamics.

Keywords: Kuramoto model, phase chaos, synchronization.

1. Introduction

Phase dynamics in ensembles of limit cycle oscillators with weak global coupling are described by the Kuramoto model [Winfree, 1980; Kuramoto, 1984]

$$\dot{\psi}_i = \omega_i + \frac{K}{N} \sum_{j=1}^N \sin(\psi_j - \psi_i), \quad i = 1, \dots, N, \quad (1)$$

where $0 \leq \psi_i < 2\pi$ are phase variables, ω_i are natural frequencies of individual oscillators, and $K > 0$ is a coupling parameter. The Kuramoto model is a generic network model [Strogatz, 2000, 2001], which is significant for numerous applications in various disciplines in the natural sciences and medicine, e.g. Josephson junction arrays [Wiesenfeld *et al.*, 1996], semiconductor lasers arrays [Kozyreff *et al.*, 2000], coupled chemical reactions [Kiss & Hudson, 2001; Kiss *et al.*, 2002], and cardiac pacemaker cells [Peskin, 1975]. The hallmark of several neurological

diseases, such as Parkinson's disease, is pathologically strong synchronization of particular populations of oscillatory neurons, which, under healthy conditions, are supposed to fire in an uncorrelated manner [Nini *et al.*, 1995]. Novel desynchronizing deep brain stimulation techniques for the therapy of such diseases [Tass, 1999] have been developed by means of an extended Kuramoto model, where a phase-dependent stimulation term was added to model electrical stimulation [Tass, 1999]. In the meantime, one of these techniques, multisite coordinated reset simulation [Tass, 2003], has been proven to be effective in a first clinical study (during depth electrode implantation) [Tass *et al.*, 2005]. This underlines the clinical relevance of studying spontaneous dynamics and control processes in the Kuramoto model. A deeper understanding of nonsynchronized states of the Kuramoto model may contribute to a further improvement of

such stimulation techniques. Hence, in this paper we study fundamental dynamical properties of the Kuramoto model emerging in the absence of synchronization.

It is known [Kuramoto, 1984; Strogatz, 2000] that the Kuramoto model exhibits incoherent behavior for small and intermediate values of the coupling coefficient K , and a spontaneous transition to collective synchronization as K exceeds a certain threshold K_c . In spite of numerous studies during the last two decades, being mainly based on a statistical approach in the thermodynamic limit $N \rightarrow \infty$, the low-dimensional and finite-dimensional dynamics of Eq. (1) is still far from being understood [Strogatz, 2000]. Our goal is to study the Kuramoto model (1) from the point of view of nonlinear dynamics of low-dimensional dynamical systems.

If the coupling $K = 0$, then $\dot{\psi}_i = \omega_i$, $i = 1, \dots, N$, and hence, the uncoupled dynamics exhibits periodic or quasiperiodic rotations on the N -dimensional torus \mathbb{T}^N . With an increase of K beyond zero, the regular dynamics undergoes perturbations and becomes chaotic. As we have found by numerical simulations, chaos in the Kuramoto model (1) appears beginning from dimension $N = 4$ [Maistrenko *et al.*, 2005; Popovych *et al.*, 2005]. It is detected in this case in a large region of parameters. Moreover, the transition to chaos is found to occur in accordance with the famous Afraimovich–Shilnikov torus destruction scenario [Afraimovich & Shilnikov, 1991; Arnold *et al.*, 1994].

It is worth noting that the behavior of the Kuramoto model for small $K > 0$ is difficult to resolve with numerical calculations. If $K < 0.1$ or so, the Lyapunov exponents appear to be very small and require much calculation time, see also [Topaj & Pikovsky, 2002]. The mathematical problem about perturbations of the uncoupled dynamics of system (1) on the torus \mathbb{T}^N is similar to the KAM theory but with the difference that the perturbations according to Eq. (1) are dissipative.

The Kuramoto model (1) as a system of N ordinary differential equations has an integral

$$\frac{1}{N} \sum_{i=1}^N \psi_i = \Omega t + C, \quad (2)$$

where Ω is the mean frequency:

$$\Omega = \frac{1}{N} \sum_{i=1}^N \omega_i, \quad (3)$$

and C is an arbitrary constant. Relation (2) implies that the mean frequency is an invariant of the Kuramoto model. It does not change its value with time and is independent of parameter K , being defined only by the natural frequencies ω_i .

Equation (1) is invariant with respect to a change of variables $\psi_i \mapsto \psi_i + \Omega t$, which reduces the mean frequency to zero. New natural frequencies are obtained by the subtraction $\omega_i - \Omega$. Therefore, it can be assumed $\Omega = 0$. Then, according to Eq. (2), C is the mean phase. Further, by shifting the variables $\psi_i \mapsto \psi_i + C$ the mean phase is reduced to zero, too. Therefore, to analyze the Kuramoto model (1), without loss of generality one can consider the case, where both mean frequency and mean phase are zero: $\Omega = 0$, $C = 0$. Any other case can be reduced to this one by the variable transformation $\psi_i \mapsto \psi_i + \Omega t + C$, which does not change the form of Eq. (1). In addition, with the use of integral (2), the dimension of the considered system (1) can be reduced by one. Indeed, let us introduce phase difference variables $\varphi_i = \psi_{i+1} - \psi_1$, $i = 1, \dots, N - 1$. By successive subtraction of the first equation in Eq.(1) from the others, one obtains that the new difference variables φ_i satisfy the following equations:

$$\dot{\varphi}_i = \Delta_i + \frac{K}{N} \left(\sum_{j=1}^{N-1} [\sin(\varphi_j - \varphi_i) - \sin(\varphi_j)] - \sin(\varphi_i) \right), \quad (4)$$

where $\Delta_i = \omega_{i+1} - \omega_1$, $i = 1, \dots, N - 1$. System (4) together with the integral (2) is equivalent to Eq. (1). Therefore, an effective dynamics of the Kuramoto model is $(N - 1)$ -dimensional. It is given by a smooth flow on an $(N - 1)$ -dimensional torus \mathbb{T}^{N-1} governed by Eq. (4). We denote this flow by Φ .

An essential characteristic of the Kuramoto model is the distribution of the natural frequencies ω_i of the individual oscillators. In the statistical theory of the Kuramoto model, operating with large $N \gg 1$, ω_i are given by a probability density function $g(\omega)$ [Kuramoto, 1984]. The function $g(\omega)$ is often assumed to be unimodal and symmetric with respect to the mean frequency Ω , i.e. $g(\Omega + \omega) = g(\Omega - \omega)$ for all ω . The frequency distribution g can, e.g. be Gaussian, Lorentzian, or a uniform distribution, see [Strogatz, 2000] for an excellent survey. In this way we come to the notion of the symmetric Kuramoto model.

2. Symmetric Kuramoto Model. Invariant Manifold

We call the Kuramoto model (1) symmetric if the natural frequencies ω_i are symmetrically allocated around the mean frequency Ω . The symmetry condition, in the case $\Omega = 0$, reads:

$$\omega_i = -\omega_{N-i+1}, \quad i = 1, \dots, N. \quad (5)$$

The symmetric Kuramoto model has an invariant manifold \mathcal{M} :

$$\mathcal{M} = \{\psi_i = -\psi_{N-i+1}, \quad i = 1, \dots, N\}. \quad (6)$$

The manifold \mathcal{M} corresponds to identical deviations of the phase variables ψ_i and ψ_{N-i+1} from the zero mean phase $C = 0$, for any $i = 1, \dots, N$. The invariance of \mathcal{M} means that any trajectory which is initiated in the manifold will never leave it. We note here that, actually, there is a one-parameter family of the invariant manifolds, $\mathcal{M}_C = \{\psi_i - C = -(\psi_{N-i+1} - C), \quad i = 1, \dots, N\}$, each corresponding to identical deviations of ψ_i and ψ_{N-i+1} from the mean phase C . With the transformation $\psi_i \mapsto \psi_i + C$, the dynamics is reduced from \mathcal{M}_C to $\mathcal{M} = \mathcal{M}_0$ of the form (6).

The manifold \mathcal{M} represents an N_0 -dimensional torus \mathbb{T}^{N_0} embedded in the N -dimensional phase space of the Kuramoto model (1), where $N_0 = [N/2]$, ($[\cdot]$ denotes the integer part of a number). The symmetric Kuramoto model, being restricted to the manifold \mathcal{M} , is reduced to the Winfree type model [Winfree, 1980; Ariaratnam & Strogatz, 2001]:

$$\dot{\psi}_i = \omega_i - Kr \sin \psi_i, \quad i = 1, \dots, N_0, \quad (7)$$

where r is a mean-field type term:

$$r = \frac{1}{N} \sum_{j=1}^N \cos \psi_j \quad (8)$$

Let us assume, for definiteness, that all ω_i are different. Then, there are two variants for symmetric allocation of the natural frequencies ω_i around zero depending on whether N is even or odd : If N is even, i.e. $N = 2N_0$, then all $\omega_i \neq 0$; and if N is odd, i.e. $N = 2N_0 + 1$, then $\omega_{N_0+1} = 0$ which implies $\psi_{N_0+1}(t) = 0$ for $t \geq 0$. Accordingly, different systems can be obtained from Eq. (7) for the in-manifold dynamics in the even and odd

cases:

$$N = 2N_0:$$

$$\dot{\psi}_i = \omega_i - \frac{K}{N_0} \sin \psi_i \sum_{j=1}^{N_0} \cos \psi_j, \quad (9)$$

$$N = 2N_0 + 1:$$

$$\dot{\psi}_i = \omega_i - \frac{K}{2N_0 + 1} \sin \psi_i \left(2 \sum_{j=1}^{N_0} \cos \psi_j + 1 \right), \quad (10)$$

$$i = 1, \dots, N_0.$$

The Winfree type models (9) and (10) are much easier to handle for an analytical study compared to the higher-dimensional system (1), at which we started our investigation. According to the models (9) and (10), the dynamics of each phase variable ψ_i reacts on its own state through the function — $\sin \psi_i$ which is multiplied by a mean-field type function which has different form for even and odd N , respectively. Note that by renumeration of the oscillators in Eq. (1), the natural frequencies ω_i , $i = 1, \dots, N_0$, can always be chosen positive in Eqs. (9) and (10).

A restriction of the dynamics of the Kuramoto model (1) to the invariant manifold \mathcal{M} requires, that the latter is stable in the whole N -dimensional phase space of Eq. (1). In other words, the in-manifold dynamics should be stable with respect to transverse perturbations, i.e. perturbations in directions out of the manifold. The transverse stability of \mathcal{M} is controlled by the transverse Lyapunov exponents corresponding to growth or decay of the transverse perturbations. There are $N - N_0 - 1$ transverse Lyapunov exponents for the manifold \mathcal{M} . By evaluating the maximal transverse Lyapunov exponent along a typical trajectory in \mathcal{M} given by Eqs. (9) and (10), parameter regions of the transverse stability of \mathcal{M} can be obtained. Our numerical simulations show that there exists a symmetry-breaking bifurcation value $K_{\text{sb}} < K_c$, such that the dynamics in \mathcal{M} is transversely stable for all $K > K_{\text{sb}}$. Here, K_c is the bifurcation value of the synchronization transition in the Kuramoto model (1). Therefore, the synchronized behavior, which takes place for all $K > K_c$, is always restricted to the manifold \mathcal{M} . With a decrease of K beyond K_c , a desynchronization transition occurs in the form of a so-called *frequency-splitting bifurcation* [Maistrenko *et al.*, 2004]: The common frequency Ω splits into two or more different frequencies. Since $K_{\text{sb}} < K_c$, we conclude that the desynchronization transition

in the Kuramoto model takes place inside the manifold \mathcal{M} and, hence, is determined by the reduced model given by Eqs. (9) and (10).

The reduction to the Winfree model is valid for all $K > K_{\text{sb}}$ and in some cases it allows to find the frequency-splitting bifurcation moment K_c analytically. For instance, for the uniform distribution of the natural frequencies in the interval $[-1; 1]$, $\omega_i = -1 + 2(i-1)/(N-1)$, $i = 1, N$, this can be done for any dimension N of Eq. (1), $K_c = K_c(N)$ [Maistrenko *et al.*, 2005]. Moreover, in the thermodynamic limit $N \rightarrow \infty$, $K_c(N)$ converges to Kuramoto's critical bifurcation value $K_{c,\infty} = 4/\pi$ [Kuramoto, 1984] and the convergence scales as $1/N$ as $N \rightarrow \infty$ [Popovych *et al.*, 2005].

3. Simplest Example: $N = 2$

Let us consider the case of only two coupled phase oscillators given by the Kuramoto model (1) with $N = 2$:

$$\begin{aligned}\dot{\psi}_1 &= \omega_1 + \frac{K}{2} \sin(\psi_2 - \psi_1), \\ \dot{\psi}_2 &= \omega_2 + \frac{K}{2} \sin(\psi_1 - \psi_2).\end{aligned}\quad (11)$$

Two phases ψ_1 and ψ_2 are called synchronized if their difference $\varphi(t) = \psi_2(t) - \psi_1(t)$ is bounded for $t > 0$. The phase difference $\varphi(t)$ clearly satisfies the following scalar equation:

$$\dot{\varphi} = \Delta - K \sin \varphi, \quad (12)$$

where $\Delta = \omega_2 - \omega_1$. The difference $\varphi(t)$ is bounded, if and only if Eq. (12) has fixed points. The synchronization is destroyed when the fixed point disappears. Clearly, there are two fixed points, $\phi^{(s)} = \arcsin(\Delta/K)$ (stable) and $\phi^{(u)} = \pi - \arcsin(\Delta/K)$ (unstable) for Eq. (12). They exist if and only if $K \geq \Delta$. Therefore,

$$K_c = \Delta$$

is a critical bifurcation value of the desynchronization transition in system (11). Indeed, for $K \geq K_c$ all solutions of Eq. (12) are asymptotically constant. Hence, both phase variables ψ_1 and ψ_2 of system (11) eventually rotate with the same average frequency $\Omega = (\omega_1 + \omega_2)/2$. For $K < K_c$ averaged frequencies $\bar{\omega}_i = \langle \dot{\psi}_i \rangle$, $i = 1, 2$, of the phase variables ψ_1 and ψ_2 are different:

$$\bar{\omega}_{1,2} = \Omega \pm \pi \left(\int_0^{2\pi} \frac{d\varphi}{\Delta - K \sin(\varphi)} \right)^{-1}.$$

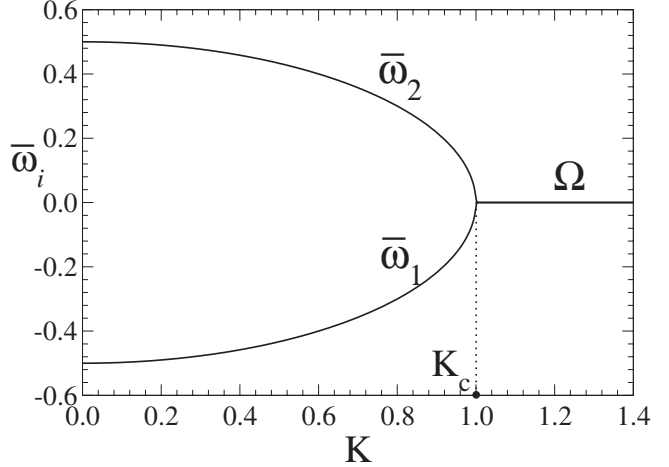


Fig. 1. Frequency-splitting bifurcation diagram for the Kuramoto model from Eq. (1) with $N = 2$ phase oscillators. The natural frequencies $\omega_1 = -0.5$ and $\omega_2 = 0.5$. $\bar{\omega}_i = \langle \dot{\psi}_i \rangle$, where $\langle \cdot \rangle$ denotes averaging over time. Ω is the mean frequency.

The desynchronization transition at $K = K_c$ is called a frequency-splitting bifurcation. Note that, as K tends to zero, the average frequencies $\bar{\omega}_1$ and $\bar{\omega}_2$ approach the natural frequencies ω_1 and ω_2 of the individual oscillators. A typical bifurcation diagram is presented in Fig. 1.

4. Simplest Nontrivial Example: $N = 3$

Let us consider the three-dimensional Kuramoto model

$$\begin{aligned}\dot{\psi}_1 &= \omega_1 + \frac{K}{3} [\sin(\psi_2 - \psi_1) + \sin(\psi_3 - \psi_1)], \\ \dot{\psi}_2 &= \omega_2 + \frac{K}{3} [\sin(\psi_1 - \psi_2) + \sin(\psi_3 - \psi_2)], \\ \dot{\psi}_3 &= \omega_3 + \frac{K}{3} [\sin(\psi_1 - \psi_3) + \sin(\psi_2 - \psi_3)].\end{aligned}\quad (13)$$

As for the case $N = 2$, there exists a bifurcation value $K = K_c$, where a desynchronization transition occurs. When parameter K decreases below K_c the common averaged frequency $\Omega = \bar{\omega}_1 = \bar{\omega}_2 = \bar{\omega}_3$, $\bar{\omega}_i = \langle \dot{\psi}_i \rangle$, $i = 1, 2, 3$, splits by producing two or three different frequencies. The course of the splitting depends on the ratio of the differences of the natural frequencies ω_1 , ω_2 , and ω_3 [Maistrenko *et al.*, 2005]. The mechanism of the frequency-splitting bifurcation can be unfolded by considering the reduced two-dimensional system of the phase differences $\varphi_1 = \psi_2 - \psi_1$

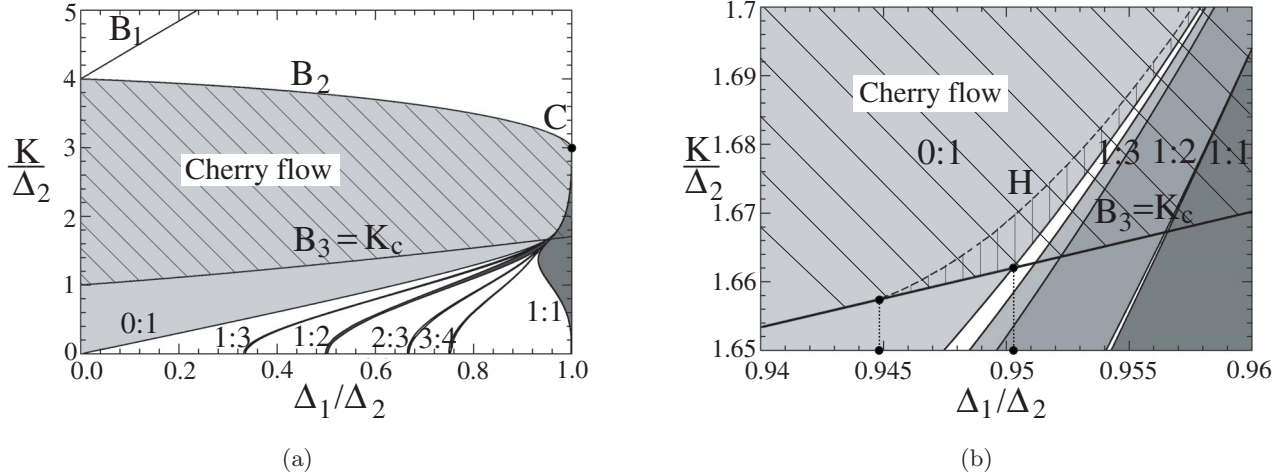


Fig. 2. (a) Two-parameter bifurcation diagram for Eq. (1) with $N = 3$. The Cherry flow region is hatched. The main resonant tongues $0:1$, $1:3$, $1:2$, $2:3$, $3:4$, and $1:1$ are shown. (b) Enlargement from (a).

and $\varphi_2 = \psi_3 - \psi_2$:

$$\begin{aligned}\dot{\varphi}_1 &= \Delta_1 + \frac{K}{3}[\sin(\varphi_2) - \sin(\varphi_1 + \varphi_2) - 2\sin(\varphi_1)], \\ \dot{\varphi}_2 &= \Delta_2 + \frac{K}{3}[\sin(\varphi_1) - \sin(\varphi_1 + \varphi_2) - 2\sin(\varphi_2)],\end{aligned}\quad (14)$$

where $\Delta_1 = \omega_2 - \omega_1$ and $\Delta_2 = \omega_3 - \omega_2$. System (14) defines a flow Φ on the two-dimensional torus $\mathbb{T}^2 = [0; 2\pi]^2$.

If $\Delta_1 = \Delta_2 \stackrel{\text{def}}{=} \Delta > 0$, the Kuramoto model is symmetric and, hence, has the invariant manifold \mathcal{M} which is simply the main diagonal $\{\varphi_1 = \varphi_2\}$. The dynamics in the manifold is governed by a scalar equation

$$\dot{\varphi} = \Delta - \frac{K}{3}[\sin(\varphi) + \sin(2\varphi)], \quad (15)$$

where $\varphi \stackrel{\text{def}}{=} \varphi_1 = \varphi_2$. The in-manifold dynamics is transversely stable for all $K > 0$.

In Fig. 2, a general bifurcation diagram for the two-dimensional torus flow Φ given by Eq. (14) is presented in the $(K/\Delta_2, \Delta_1/\Delta_2)$ -parameter plane. For large values of K flow Φ has six fixed points: one stable node, two unstable nodes and three saddles. With decreasing K the fixed points annihilate in pairs at three saddle-node bifurcation curves B_i , $i = 1, 2, 3$. A Cherry flow [Cherry, 1938; Boyd, 1985; Veerman, 1989; Baesens *et al.*, 1991] exists between the second and the third bifurcation curves B_2 and B_3 , where only two fixed points, the stable

node and one of the saddles are left. According to [Baesens *et al.*, 1991] a Cherry flow is a smooth flow on a two-dimensional torus, which has two equilibria, one being a saddle and the other being a sink or source, and rotating trajectories of some rotation number called winding ratio. The frequency-splitting occurs when the parameter point crosses curve B_3 . The enlargement in Fig. 2(b) shows that the Cherry flow resonant tongues are naturally continued into the desynchronization region below B_3 .

The Cherry flow resonant tongues contain thin boundary layer strips, where a stable periodic orbit exists. The periodic orbit is born at a homoclinic bifurcation of the saddle. One of the homoclinic bifurcation curves is shown in Fig. 2(b) as a dashed line H inside the $0:1$ tongue.

For more details on Eq. (14) and the three-dimensional Kuramoto model (13) see [Maistrenko *et al.*, 2004; Maistrenko *et al.*, 2005].

5. Chaotic Attractor in the Kuramoto Model: $N = 4$

In this section we demonstrate the emergence of a chaotic attractor in the four-dimensional Kuramoto model

$$\dot{\psi}_i = \omega_i + \frac{K}{4} \sum_{j=1}^4 \sin(\psi_j - \psi_i), \quad i = 1, \dots, 4. \quad (16)$$

As before, by introducing the phase difference variables $\varphi_i = \psi_{i+1} - \psi_i$, $i = 1, 2, 3$, system (16) is reduced to a three-dimensional system of the

form:

$$\begin{aligned}\dot{\varphi}_1 &= \Delta_1 - \frac{K}{4}[2\sin(\varphi_1) + \sin(\varphi_1 + \varphi_2) \\ &\quad + \sin(\varphi_1 + \varphi_2 + \varphi_3) - \sin(\varphi_2) \\ &\quad - \sin(\varphi_2 + \varphi_3)], \\ \dot{\varphi}_2 &= \Delta_2 - \frac{K}{4}[2\sin(\varphi_2) + \sin(\varphi_1 + \varphi_2) \\ &\quad + \sin(\varphi_2 + \varphi_3) - \sin(\varphi_1) - \sin(\varphi_3)], \\ \dot{\varphi}_3 &= \Delta_3 - \frac{K}{4}[2\sin(\varphi_3) + \sin(\varphi_2 + \varphi_3) \\ &\quad + \sin(\varphi_1 + \varphi_2 + \varphi_3) - \sin(\varphi_2) \\ &\quad - \sin(\varphi_1 + \varphi_2)],\end{aligned}\tag{17}$$

where $\Delta_i = \omega_{i+1} - \omega_i$, $i = 1, 2, 3$. Therefore, the dynamics of system (16) is given by a smooth flow Φ on the three-dimensional torus \mathbb{T}^3 .

The Kuramoto model is symmetric if $\Delta_1 = \Delta_3$. In this case, it has a symmetric invariant manifold $\mathcal{M} = \{\varphi_1 = \varphi_3\}$. The dynamics in the manifold is two-dimensional and given by the system

$$\begin{aligned}\dot{\varphi}_1 &= \Delta_1 - \frac{K}{4}[2\sin(\varphi_1) + \sin(2\varphi_1 + \varphi_2) - \sin(\varphi_2)], \\ \dot{\varphi}_2 &= \Delta_2 - \frac{K}{2}[\sin(\varphi_2) + \sin(\varphi_1 + \varphi_2) - \sin(\varphi_1)].\end{aligned}\tag{18}$$

The general bifurcation diagram for the system (18) in the $(K/\Delta_2, \Delta_1/\Delta_2)$ -parameter plane

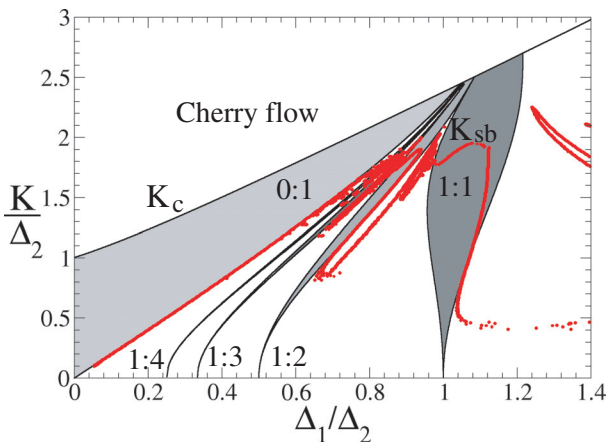


Fig. 3. Two-parameter bifurcation diagram for Eq. (18). The main resonant tongues $0:1$, $1:4$, $1:3$, $1:2$, and $1:1$ are shown. Red points indicate a symmetry-breaking bifurcation curve K_{sb} of the manifold \mathcal{M} .

is presented in Fig. 3. As one can see, the symmetry-breaking bifurcation curve K_{sb} lies below the synchronization transition curve K_c . The in-manifold dynamics is transversely stable above K_{sb} and is transversely unstable below K_{sb} . Therefore, the desynchronization transition at $K = K_c$ takes place inside the manifold \mathcal{M} . Above the bifurcation curve K_c the in-manifold dynamics is given by a Cherry flow. In Fig. 3, the resonant tongues of the two-dimensional flow given by Eq. (18) are shown. The structure of the resonant tongues is analogous to the tongues from Fig. 2, but there is no symmetry with respect to $\Delta_1/\Delta_2 = 1$.

The desynchronization transition and the emergence of chaos in the Kuramoto model (16) are shown in Figs. 4 and 5 for the parameter values that vary along the vertical parameter line $\Delta_1/\Delta_2 = 1$ in Fig. 3. Three Lyapunov exponents λ_1 , λ_2 and λ_3 of the reduced system (17) are plotted in Fig. 5. The desynchronization occurring at $K_c \approx 2.37$ takes place inside the $0:1$ resonant tongue (Fig. 3). The common mean frequency $\Omega = \bar{\omega}_1 = \bar{\omega}_2 = \bar{\omega}_3 = \bar{\omega}_4$ splits into two different average frequencies $\bar{\omega}_1 = \bar{\omega}_2$ and $\bar{\omega}_3 = \bar{\omega}_4$ (Fig. 4), where $\bar{\omega}_i = \langle \dot{\psi}_i \rangle$ and $\langle \cdot \rangle$ denotes averaging over time.

The desynchronization transition at $K = K_c$ takes place via a saddle-node bifurcation: The only stable equilibrium of system (17) collides with a saddle, in this way producing a stable limit cycle $P_{0:1:0} \in \mathcal{M}$ with rotation number $0:1:0$, see Fig. 6(a). With a further decrease of K , the parameter point escapes from the $0:1:0$ resonant tongue

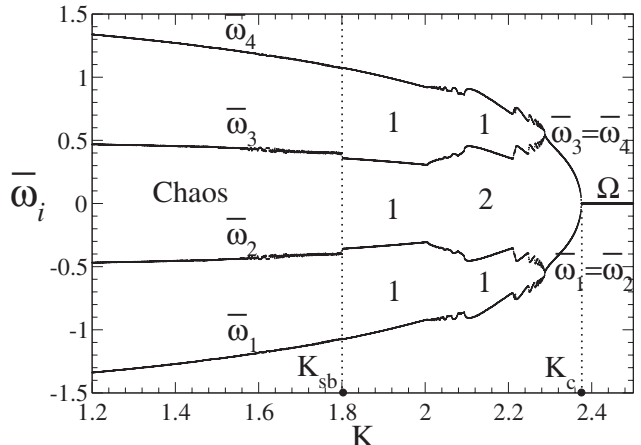


Fig. 4. Frequency-splitting bifurcation diagram for the Kuramoto model from Eq. (1) with $N = 4$ phase oscillators, with natural frequencies ω_i uniformly distributed in the interval $[-1.5; 1.5]$. $\bar{\omega}_i = \langle \dot{\psi}_i \rangle$, where $\langle \cdot \rangle$ denotes averaging over time. Ω is the mean of the natural frequencies.

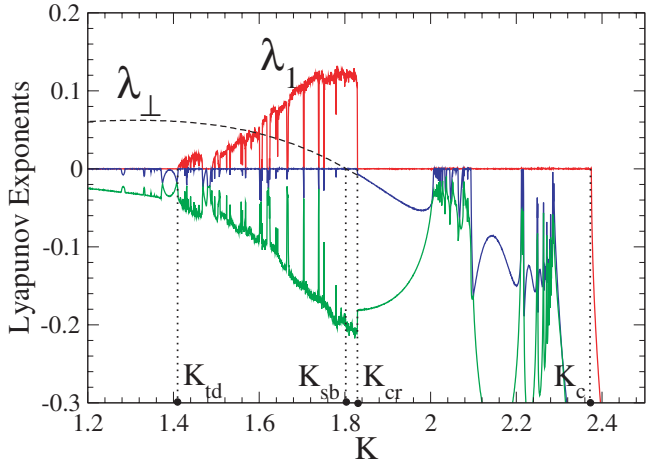


Fig. 5. Lyapunov exponents of the Kuramoto model from Eq. (1) with $N = 4$ phase oscillators, with natural frequencies ω_i uniformly distributed in the interval $[-1.5; 1.5]$.

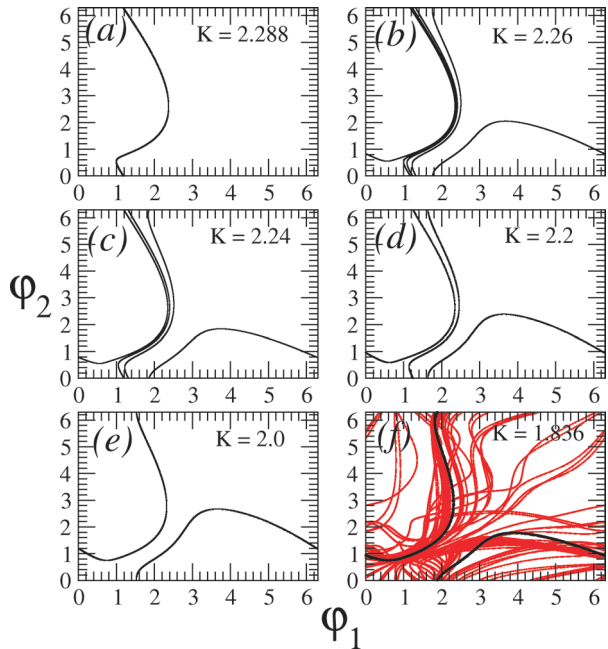


Fig. 6. Stable limit states of system (17) for different values of coupling parameter K and for $\Delta_1 = \Delta_2 = \Delta_3 = 1$. In (a)–(e) the resonant dynamics within the manifold \mathcal{M} is shown. In (f) the coexistence of stable limit cycle $P_{1:1:1} \in \mathcal{M}$ (black dots) and a chaotic attractor $A \notin \mathcal{M}$ (red dots) is illustrated.

and crosses infinitely many narrow resonant tongues with rotation numbers $1:q:1$. In Figs. 6(b)–6(d) the corresponding limit cycles with rotation numbers $1:4$, $1:3$ and $1:2$ are shown. Finally, the parameter point enters the main $1:1:1$ -resonant tongue, where a stable limit cycle $P_{1:1:1}$ with rotation number $1:1:1$ exists [Fig. 6(e)]. Note that there are regions of quasiperiodicity, where two Lyapunov

exponents equal zero, in between the $1:q:1$ resonant tongues. The quasiperiodic regions are filled by extremely narrow tongues of high-resonance periodic dynamics, see Figs. 4 and 5.

The periodic and the quasiperiodic dynamics mentioned above takes place within the symmetric invariant manifold \mathcal{M} . The two-dimensional invariant manifold is transversally stable up to the symmetry-breaking bifurcation point $K_{\text{sb}} \approx 1.8$. At the bifurcation, the limit cycle $P_{1:1:1} \in \mathcal{M}$ loses its stability in the transverse to the manifold direction, see graph of the transverse Lyapunov exponent λ_\perp in Fig. 5. Nevertheless, $P_{1:1:1}$ preserves the in-manifold stability for all $K > 0$, as it can be concluded from Fig. 3.

As demonstrated in Fig. 5, the maximal Lyapunov exponent λ_1 is positive for values of K between $K_{\text{td}} \approx 1.41$ and $K_{\text{cr}} \approx 1.83$, which implies an existence of a chaotic attractor A . The chaotic attractor A is born, at $K = K_{\text{td}}$, in accordance with the Afraimovich–Shilnikov torus destruction scenario [Afraimovich & Shilnikov, 1991; Arnold *et al.*, 1994] of the transition to chaos. At $K = K_{\text{cr}}$, A is destroyed in a boundary crises transforming into a chaotic saddle. The chaotic interval $(K_{\text{td}}, K_{\text{cr}})$ is filled with windows of periodicity.

Before the chaotic attractor A is born, i.e. for $K < K_{\text{td}}$, the system dynamics is mostly quasiperiodic and is restricted to a two-dimensional nonresonant torus \mathbb{T}_{nr}^2 . An example of a Poincaré section of the torus is shown in Fig. 7(a) for $K = 1.37$. At $K = K_{\text{sn}} \approx 1.372$, the torus dynamics fits in a wide enough window of periodicity, see Fig. 5. At the transition from the nonresonant torus \mathbb{T}_{nr}^2 to the resonant torus \mathbb{T}_r^2 a stable periodic orbit P (shown by square symbols in Fig. 7(a) for $K = 1.41$) and a saddle Q of the rotation number $9:10:9$ are born in a saddle-node bifurcation at $K = K_{\text{sn}}$. Geometrically, the resonant torus \mathbb{T}_r^2 is a closure of the unstable manifolds of the saddle Q . Passing through the resonance, the torus \mathbb{T}_r^2 , first, loses its smoothness. Then, when escaping from the resonant window at $K = K_{\text{td}}$, the torus \mathbb{T}_r^2 is destroyed and the chaotic attractor A is born at its place. The chaotic attractor A is shown in Figs. 7(b)–7(d). Just after its emergence, A is very thin and inherits the shape of the former torus \mathbb{T}_r^2 [Fig. 7(b)]. With a further increase of K , a fractal structure of A develops [Fig. 7(c)] and becomes clearly visible [Fig. 7(d)]. Finally, at $K = K_{\text{cr}}$ A undergoes a boundary crisis and transforms into a chaotic saddle.

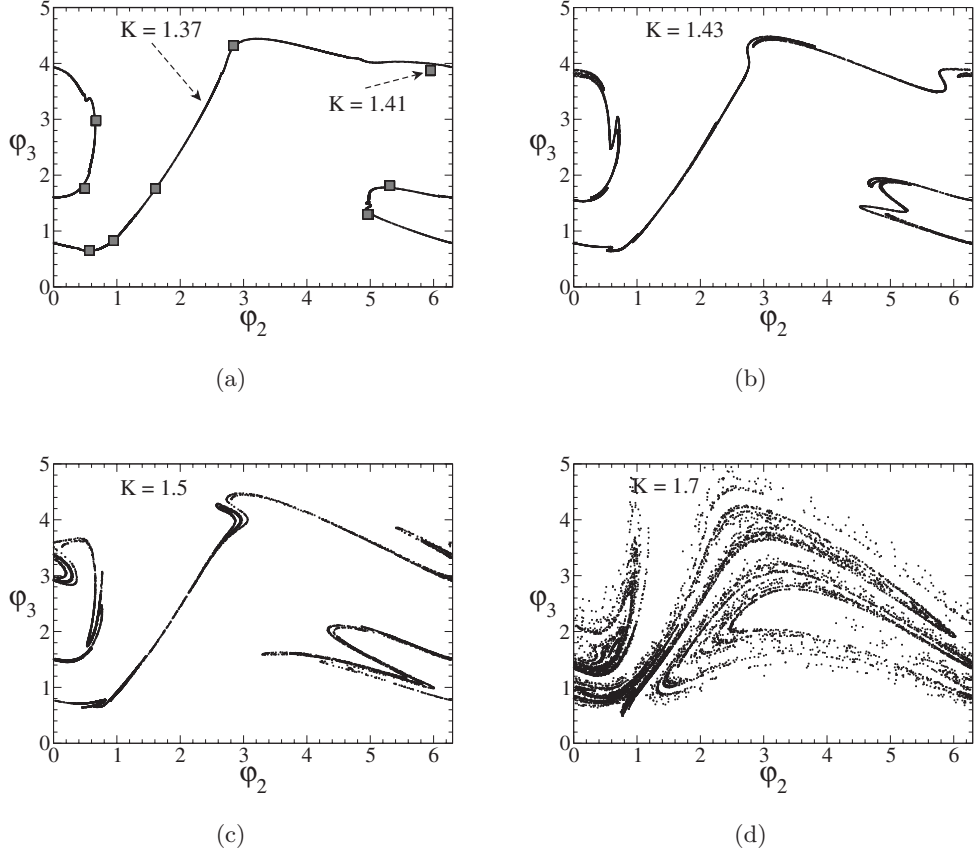


Fig. 7. Poincaré section at $\varphi_1 = 0$ for the system in differences (17) for different values of coupling parameter K and for $\Delta_1 = \Delta_2 = \Delta_3 = 1$. In (a) a nonresonant two-torus and a resonant two-torus are shown. In (b)–(d) a chaotic attractor A is depicted.

After the attractor crisis at $K = K_{\text{cr}}$, the dynamics drops down to a stable periodic orbit $P_{1:1:1} \in \mathcal{M}$ of the main resonance $1:1:1$. As one can see from Fig. 5, the symmetry-breaking bifurcation value K_{sb} lies to the left of the value K_{cr} . Hence, two attractors coexist in the coupling parameter interval between K_{sb} and K_{cr} : the chaotic attractor A and the stable periodic orbit $P_{1:1:1}$. The multistability phenomenon is illustrated in Fig. 6(f).

In Fig. 8 a general bifurcation diagram for the four-dimensional Kuramuro model (16) is presented. The parameter plane is the same as in Fig. 3, but here the three-dimensional dynamics is also indicated. Different colors correspond to different limiting behavior in the system, which is detected with the use of the Lyapunov exponents. The phase chaos region ($\lambda_1 > 0$) is colored in red. Another region, where a stable limit cycle exists ($\lambda_1 = 0$, $\lambda_2 < 0$, and $\lambda_3 < 0$) is shown in blue. One more region, with a stable two-torus dynamics ($\lambda_1 = \lambda_2 = 0$ and $\lambda_3 < 0$) is colored in green. Finally, the

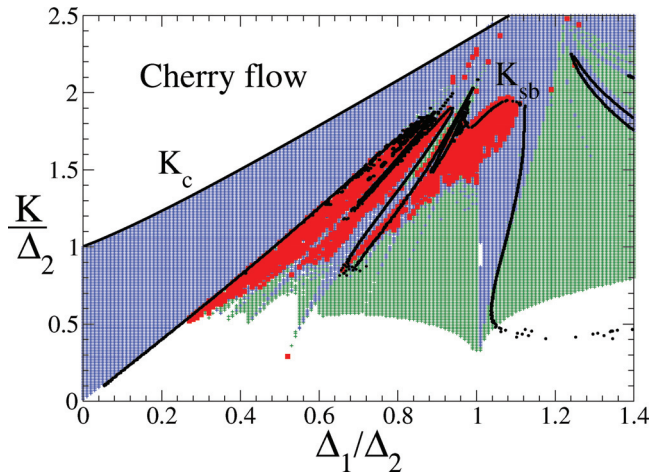


Fig. 8. Regions in $(K/\Delta_2, \Delta_1/\Delta_2)$ -parameter plane of different stable dynamical regimes of the system in differences (17) for $\Delta_3 = \Delta_1$. Blue points indicate stable limit cycle, green points indicate two-dimensional torus \mathbb{T}^2 , and red points indicate chaotic dynamics. Black dots mark the bifurcation curves of the desynchronization transition K_c and the symmetry-breaking bifurcation K_{sb} , respectively.

region where all three Lyapunov exponents almost vanish (up to the precision $|\lambda_i| < 0.0005$, $i = 1, 2, 3$) for small values of the coupling parameter K is left blank.

The three-dimensional chaotic dynamics, as one can see in Fig. 8, also extends above the curve K_{sb} (black dots). It indicates regions of multistability, i.e. coexistence of the three-dimensional attractor with the two-dimensional symmetric attractor in the manifold \mathcal{M} . The phase chaos region (red) is mostly concentrated between regions of periodicity (blue) and quasiperiodicity (green). The typical scenario of the transition to chaos was described above for the case $\Delta_1/\Delta_2 = 1$.

6. Discussions

Phase chaos is a general phenomenon of the Kuramoto model (1). Indeed, analogous chaotic phase dynamics, with one positive LE is found in the Kuramoto model (1) of dimension $N = 5$. The behavior becomes hyperchaotic for $N = 6$ and $N = 7$, where two Lyapunov exponents attain positive values, which again holds for a large coupling parameter interval [Maistrenko *et al.*, 2005]. Generally, our numerical experiments show that phase chaos is an essential property of the N -dimensional Kuramoto model, and it is characterized by $(N - 2)/2$ (N even) or $(N - 3)/2$ (N odd) positive Lyapunov exponents. Moreover, the Lyapunov exponents are scaled quadratically with K , as K vanishes, and are scaled inverse proportionally to N , as N grows [Popovych *et al.*, 2005].

Phase chaos is by no means restricted to the Kuramoto model (1). Rather, it also occurs in globally coupled limit cycle oscillators and Rössler systems [Popovych *et al.*, 2005]. Also, phase chaos has been detected in term of positive LEs in previous studies of phase oscillators with nearest-neighboring coupling [Topaj & Pikovsky, 2002] and coupled Lorenz systems [Liu *et al.*, 2003]. This strongly indicates that phase chaos is a universal behavior of coupled oscillators.

References

- Afraimovich, V. S. & Shilnikov, L. P. [1991] “Invariant two-dimensional tori, their breakdown and stochasticity,” *Amer. Math. Soc. Transl.* **149**, 201–212.
- Ariaratnam, J. T. & Strogatz, S. H. [2001] “Phase diagram for the Winfree model of coupled nonlinear oscillators,” *Phys. Rev. Lett.* **86**, 4278–4281.
- Arnold, V. I., Afraimovich, V. S., Ilyashenko, Yu. S. & Shilnikov, L. P. [1994] *Encyclopedia of Mathematical Sciences, Dynamical Systems V* (Springer-Verlag, Berlin).
- Baesens, C., Guckenheimer, J., Kim, S. & MacKay, R. S. [1991] “Three coupled oscillators: Mode-locking, global bifurcations and toroidal chaos,” *Physica* **D49**, 387–475.
- Boyd, C. [1985] “On the structure of the family of Cherry fields on the torus,” *Ergod. Th. Dyn. Syst.* **5**, 27–46.
- Cherry, T. M. [1938] “Analytic quasi-periodic curves of discontinuous type on a torus,” *Proc. London Math. Soc.* **44**, 175–215.
- Kiss, I. Z. & Hudson, J. L. [2001] “Phase synchronization and suppression of chaos through intermittency in forcing of an electrochemical oscillator,” *Phys. Rev. E* **64**, 046215.
- Kiss, I. Z., Zhai, Y. & Hudson, J. L. [2002] “Collective dynamics of chaotic chemical oscillators and the law of large numbers,” *Phys. Rev. Lett.* **88**, 238301.
- Kozyreff, G., Vladimorov, A. G. & Mandel, P. [2000] “Global coupling with time delay in an array of semiconductor lasers,” *Phys. Rev. Lett.* **85**, 3809–3812.
- Kuramoto, Y. [1984] *Chemical Oscillations, Waves and Turbulence* (Springer-Verlag, Berlin).
- Liu, Z., Lai, Y.-C. & Matias, M. A. [2003] “Universal scaling of Lyapunov exponents in coupled chaotic oscillators,” *Phys. Rev. E* **67**, 045203(R).
- Maistrenko, Yu., Popovych, O., Burylko, O. & Tass, P. A. [2004] “Mechanism of desynchronization in the finite-dimensional Kuramoto model,” *Phys. Rev. Lett.* **93**, 84102.
- Maistrenko, Yu. L., Popovych, O. V. & Tass, P. A. [2005] *Desynchronization and Chaos in the Kuramoto Model*, Lectures Notes in Physics, Vol. 671, pp. 285–306.
- Nini, A., Feingold, A., Slovin, H. & Bergmann, H. [1995] “Neurons in the globus pallidus do not show correlated activity in the normal monkey, but the phase-locked oscillations appear in the MRTP model of parkinsonism,” *J. Neurophysiol.* **74**, 1800–1805.
- Peskin, C. S. [1975] *Mathematical Aspects of Heart Physiology* (Courant Institute of Mathematical Sciences, NY).
- Popovych, O. V., Maistrenko, Yu. L. & Tass, P. A. [2005] “Phase chaos in coupled oscillators,” *Phys. Rev. E* **71** 065201(R).
- Strogatz, S. H. [2000] “From Kuramoto to Crawford: Exploring the onset of synchronization in populations of coupled oscillators,” *Physica* **D143**, 1–20.
- Strogatz, S. H. [2001] “Exploring complex networks,” *Nature (London)* **410**, 268–276.
- Tass, P. A. [1999] *Phase Resetting in Medicine and Biology. Stochastic Modelling and Data Analysis* (Springer, Berlin).

- Tass, P. A. [2003] “A model of desynchronizing deep brain stimulation with a demand-controlled coordinated reset of neural subpopulations,” *Biol. Cybern.* **89**, 81–88.
- Tass, P. A., Russell, D. F., Barnikol, U. B., Neiman, A. B., Yakusheva, T. A., Hauptmann, C., Voges, J., Sturm, V. & Freund, H.-J. [2005] “Selective disruption of neural synchronization by means of multisite transient phase reset,” submitted.
- Topaj, D. & Pikovsky, A. [2002] “Reversibility versus synchronization in oscillator lattices,” *Physica D* **170**, 118–130.
- Veerman, J. J. P. [1989] “Irrational rotation numbers,” *Nonlinearity* **2**, 419–428.
- Wiesenfeld, K., Colet, P. & Strogatz, S. H. [1996] “Synchronization transitions in a disordered Josephson series array,” *Phys. Rev. Lett.* **76**, 404–407.
- Winfree, A. T. [1980] *The Geometry of Biological Times* (Springer, NY).